Applied Catalysis B: Environmental 90 (2009) 485–488

Contents lists available at ScienceDirect

Applied Catalysis B: Environmental

journal homepage: www.elsevier.com/locate/apcatb

Carbon dioxide reforming of ethanol over $Ni/Y_2O_3–ZrO_2$ catalysts

Jorge D.A. Bellido, Eurico Y. Tanabe, Elisabete M. Assaf*

Instituto de Química de São Carlos, Universidade de São Paulo, Av. Trabalhador Sãocarlense, 400, 13560-970 São Carlos, SP, Brazil

ARTICLE INFO

Article history:
Received 16 December 2008
Received in revised form 26 March 2009
Accepted 6 April 2009
Available online 16 April 2009

Keywords:
Dry reforming of ethanol
$Ni/Y_2O_3–ZrO_2$
Catalyst preparation

ABSTRACT

Supported nickel catalysts of composition $Ni/Y_2O_3–ZrO_2$ were synthesized in one step by the polymerization method and compared with a nickel catalyst prepared by wet impregnation. Stronger interactions were observed in the formed catalysts between NiO species and the oxygen vacancies of the $Y_2O_3–ZrO_2$ in the catalysts made by polymerization, and these were attributed to less agglomeration of the NiO during the synthesis of the catalysts in one step. The dry reforming of ethanol was catalyzed with a maximum CO_2 conversion of 61% on the 5NiYZ catalyst at 800 °C, representing a better response than for the catalyst of the same composition prepared by wet impregnation.

1. Introduction

In the last two decades, the use of ethanol as a potential substitute for fossil fuels has expanded greatly, as it is renewable and environmentally friendly. Most of the research in this area focuses on steam reforming of ethanol. Other ways to produce hydrogen from ethanol include the partial oxidation of ethanol [1,2]. Various catalysts based on noble metals [2] and transitions metals [3,4] have been used in the production of hydrogen from ethanol and among these, nickel-based catalysts are relatively cheap and active [5,6]. In addition, studies of nickel catalysts supported on ZrO_2 systems have demonstrated interesting metal–support interactions that may benefit the catalytic properties [7,8]. Concerning the dry reforming of methane, Roh et al. [9] reported that a nickel catalyst supported on $CeO_2–ZrO_2$ was more active and stable than on the respective single oxides; similarly, Srinivas et al. [10], for a similar catalyst, demonstrated good stability and activity in the steam reforming of ethanol, due to the its capacity for oxygen storage on the oxygen vacancies of the support material. The participation of the oxygen vacancies in ZrO_2 systems in catalytic processes is well established [11,12]. Although several authors have studied the performance of catalytic systems in the steam reforming of ethanol, little has been published on the dry reforming of ethanol [13]. In the context of the above discussion, this article investigates the possibility of the dry reforming of ethanol on nickel catalysts supported on $Y_2O_3–ZrO_2$ and proposes a new route to synthesis of the Ni catalyst on $Y_2O_3–ZrO_2$ in one step, by the polymerization method (Pechini).

2. Experimental

Two nickel catalysts were prepared by the polymerization method in one step from the salts $ZrO_2{\cdot}CO_2{\cdot}1.5H_2O$ (Aldrich), $Y(NO_3)_2{\cdot}6H_2O$ (Aldrich), and $Ni(NO_3)_2{\cdot}3H_2O$ (Aldrich), with a mole fraction of 12% Y_2O_3/ZrO_2, the nickel loads being 5 wt.% and 10 wt.% relative to the $Y_2O_3–ZrO_2$ mass. The general procedure for the polymerization method has been reported previously [14], but without the addition of nickel salts. Briefly, zirconium carbonate was dissolved in nitric acid and the resulting solution mixed with an aqueous solution of calcium and nickel nitrate. This solution was added to a solution of citric acid in ethylene glycol and the mixture taken to 120 °C and held at this temperature for 24 h, to bring about the polymerization. The products were dried at 110 °C for 12 h and finally calcined by heating from 25 °C to 500 °C over 3 h, at a heating rate of 2 °C min^{-1}, and later to 750 °C over 2 h, at a rate of 2 °C min^{-1}.

These catalysts were denominated 5NiYZ and 10NiYZ, for 5 wt.% and 10 wt.% nickel respectively. For the purpose of comparison, a catalyst was prepared with the same composition as 5NiYZ, by wet impregnation: 5 wt.% nickel was added, in a solution of the nitrate, to the $Y_2O_3–ZrO_2$ support and calcined at 750 °C for 2 h. This was named 5NiYZ(i). The $Y_2O_3–ZrO_2$ support (YZ) used for this was also synthesized by the polymerization method.

The specific surface area (BET) was estimated from the N_2 adsorption/desorption isotherms at liquid nitrogen temperature, using a Quantachrome NOVA 1000 version 10.02. The crystalline phases were identified with a Rigaku Multiflex diffractometer with nickel-filtered Cu Kα radiation (λ = 1.5418 Å, 40 kV/40 mA) at a scan speed of 2° min^{-1}. The average size of crystallites in the samples was determined by the Scherrer equation. Temperature-programmed

* Corresponding author. Tel.: +55 1633739951; fax: +55 1633739952.
E-mail address: eassaf@iqsc.usp.br (E.M. Assaf).

0926-3373/$ – see front matter © 2009 Published by Elsevier B.V.
doi:10.1016/j.apcatb.2009.04.009

Table 1
Physical properties of catalysts and YZ support.

Samples	Crystallite size[a] (nm)		S_{BET}[b] ($m^2\ g^{-1}$)
	Y_2O_3–ZrO_2	NiO	
YZ	7.5	–	23
5NiYZ(i)	9.4	25.9	14
5NiYZ	8.3	12.5	22
10NiYZ	6.8	14.3	38

[a] The maximum error using the Scherrer formula is 4% [15].
[b] The standard of deviation of the S_{BET} measures is 10%.

Table 2
Reduction data derived from the TPR profiles in Fig. 2.

Sample	H_2 consumption (mol H_2) × 10^5			
	α	β	$(\alpha+\beta)$	γ
YZ	–	–	–	10.2
5NiYZ(i)	2.4	7.8	10.2	9.1
5NiYZ	8.3	1.1	9.4	9.5
10NiYZ	8.0	10.2	18.2	5.5

reduction (TPR) was performed with a multipurpose analytical system (SAMP3, Termolab Equipamentos Ltd., Brazil) with a TCD detector, a reducing gas mixture of 5% H_2:95% He (v/v) and a heating rate of 10 °C min^{-1}.

Catalytic reactions were carried out in a fixed-bed down-flow quartz reactor (i.d. = 10 mm) connected in-line to a gas chromatograph fitted with a TCD. The catalysts (100 mg) were activated by reducing them with H_2 (30 mL h^{-1}) at 700 °C for 1 h. The feed of CO_2/C_2H_5OH was in the molar ratio 1:1, the ethanol being fed at a flow rate of 1.3 mL h^{-1}.

3. Results and discussion

Table 1 summarizes the BET surface areas and the mean crystallite sizes of the 5NiYZ, 10NiYZ and 5NiYZ(i) catalysts and of the YZ support and their XRD patterns are shown in Fig. 1. The presence of NiO and of the tetragonal phase of Y_2O_3–ZrO_2 [JCPDS 17-923] was identified in the XRD patterns of the catalysts. There were also weak diffraction peaks of the monoclinic phase of ZrO_2 in the 5NiYZ(i) catalyst. These differences may be attributed to differences in the synthesis method. The reason for choosing the polymerization method in one step, including the nickel salts, was based on the idea of distributing the cations atomistically throughout the polymer, as chelates are formed between the cations in solution and the carboxylic acid side-groups on the polymer formed by esterification of ethylene glycol and citric acid. The aim was to disperse the single cations uniformly over the polymer formed, so that, in the calcination step, the polymer would decompose to leave nanometric crystallites.

The cross-linked polymer thus provides benefits such as more homogeneous mixing of cations during charring and the calcinations [16]. On other hand, Y_2O_3 is known to be soluble in ZrO_2 and to form a solid solution with the generation of oxygen vacancies [17,18], whereas the dissolution of NiO in the Y_2O_3–ZrO_2 formed is practically zero (<1.5 mol% at 1500 °C) [19], suggesting that the NiO would form a second phase over the Y_2O_3–ZrO_2 in the less drastic calcination used in this study. Hence, it is possible to obtain similar catalysts, either by including the NiO salt directly in the polymeric synthesis of the Y_2O_3–ZrO_2 matrix, or by the NiO wet impregnation method. Y_2O_3–ZrO_2 tetragonal phase stabilization was observed in the 5NiYZ catalyst but no extra peaks related to the monoclinic ZrO_2, which were seen in the case of 5NiYZ(i) obtained by impregnation. Observing the crystallite size related to plane (1 1 1) of the Y_2O_3–ZrO_2 support, it can be seen that it is smaller in the 5NiYZ catalyst. Moreover, the crystallites of NiO are twice as large in the 5NiYZ(i) than in 5NiYZ. In the polymerization synthesis in one step, the low solubility of the NiO leads to segregation of this phase on the Y_2O_3–ZrO_2 surface, accompanied by a diminution of the surface energy that retards the growth of particles, raising the total surface area [20], as confirmed in the BET surface area measurements. Increasing the NiO load (10NiYZ catalyst) led to more particles of segregated NiO, with a higher surface area. The NiO crystallites of the 10NiYZ catalyst were smaller than those of the 5NiYZ(i), indicating that one-step synthesis led to less aggregation of the catalyst.

The TPR profiles are shown in Fig. 2 and the related data in Table 2. In a previous paper [14], we reported the participation of oxygen vacancies of the Y_2O_3–ZrO_2 support in promoting NiO reduction, shifting to lower temperatures the reduction of NiO species in contact with the oxygen vacancies. These oxygen vacancies may polarize the H_2 molecule, so that it attacks more readily the oxygen of the NiO, or the interaction between the oxygen vacancies and the oxygen of the NiO may weaken the Ni–O bond, making the oxygen easily removable [21]. In Fig. 2 there are three reduction peaks, the first two (α and β) being related to the reduction of NiO species and the third (γ) to the reduction of the YZ support.

Considering the reduction curve for the YZ support, the H_2 consumption is equivalent to 0.31% of the total ZrO_2, a low level of reduction also reported by other authors [22]. Also, a continuous shift of the γ peak to lower temperatures is observed in the

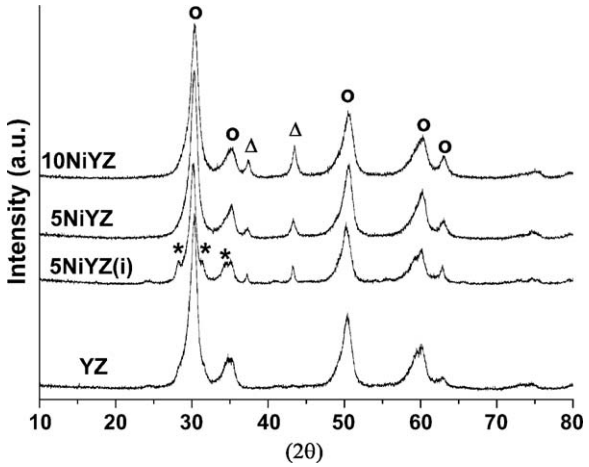

Fig. 1. XRD patterns of catalysts and YZ support. (○) Tetragonal phase, (*) monoclinic phase, and (Δ) NiO.

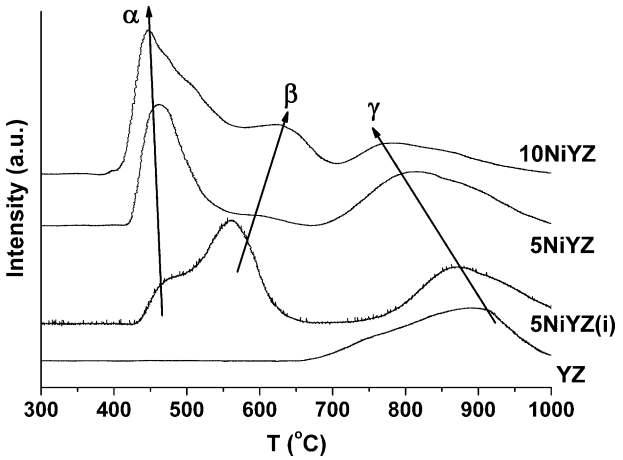

Fig. 2. TPR profiles of samples. Conditions: 10 °C min^{-1}, 100 mg sample, 5%H_2/Ar flowing at 30 mL min^{-1}.

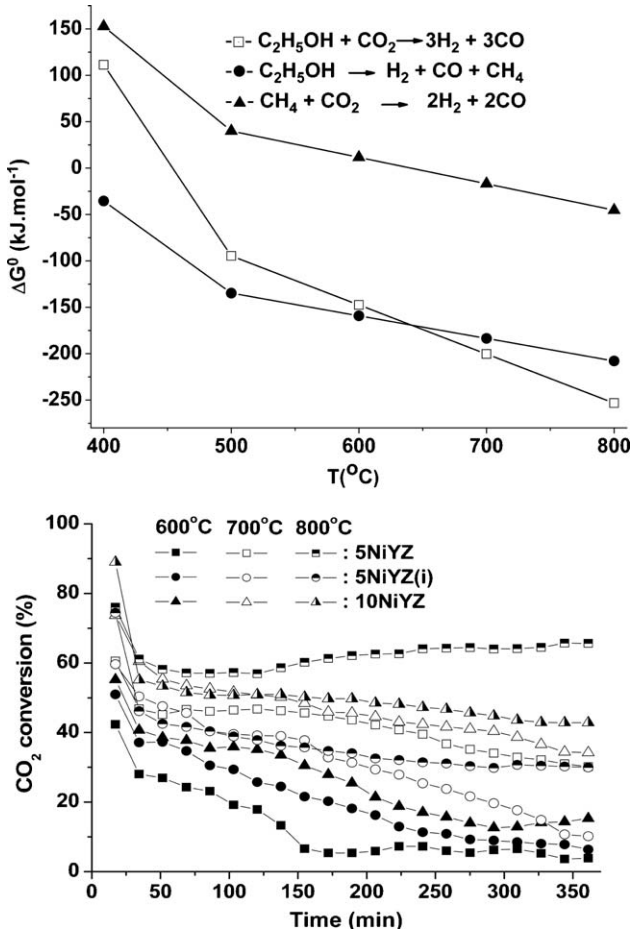

Fig. 3. (a) Gibbs free energy and (b) CO_2 conversion in the dry reforming of ethanol.

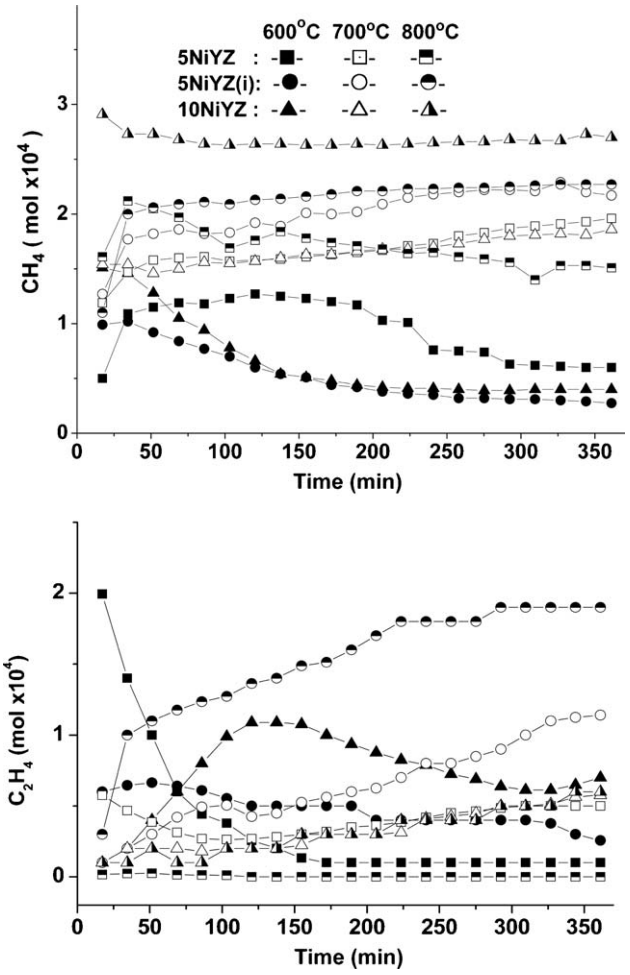

Fig. 4. (a) CH_4 and (b) C_2H_4 production in dry reforming of ethanol.

presence of Ni and this is more pronounced when the catalysts are synthesized in one step, indicating that under these conditions, more nickel interacts with the support, giving rise to a spillover effect on the reduction of the support.

The α peak was attributed to the reduction of NiO species located in the vicinity of oxygen vacancies in the supports, and the β peak to the reduction of NiO species with little interaction with the oxygen vacancies or in the form of crystallites. Considering the H_2 consumption values, a much greater reduction of NiO species is seen in the α peak for the 5NiYZ catalyst, relative to the 5NiYZ(i) catalyst, indicating a greater amount of NiO species in contact with the oxygen vacancies. This behavior may be explained by the less aggregated NiO species produced in the polymerization synthesis in one step, as greater NiO dispersion would increase the quantity of NiO being influenced by the oxygen vacancies. This is confirmed by the XRD data, which showed smaller NiO crystallites and hence less aggregation in the 5NiYZ synthesized in one step. This influence of the oxygen vacancies of the support on the NiO species in their vicinity is consistent with the TPR of the 10NiYZ catalyst, in which the α peak remained practically equal to the 5NiYZ peak, owing to the limited number of oxygen vacancies available on the YZ surface, whereas the β peak, ascribed to the NiO species with little interaction with the oxygen vacancies, increased significantly.

Figs. 3–5 and Table 3 summarize the data obtained in the dry reforming of ethanol, in the range of 600–800 °C, over 6 h.

Fig. 3 shows the thermodynamic possibility of achieving the dry reforming of ethanol via the decomposition of ethanol. However, the dry reforming of methane is permitted from approximately 640 °C, while it is possible to obtain H_2 and CO at approximately 454 °C. Also, the CO_2 conversion is shown in Fig. 3b: significantly more than approximately 40% is seen above 700 °C, increasing at 800 °C with correspondingly less carbon deposition (Table 3).

Table 3
Ethanol conversion, liquid residue formation and carbon deposition for 6 h of reaction.

Catalyst	Liquid residues (mmol)						Carbon (mmol)			Ethanol conv. (%)		
	CH_3CHO			H_2O			C			C_2H_5OH		
	600[a]	700[a]	800[a]	600[a]	700[a]	800[a]	600[a]	700[a]	800[a]	600[a]	700[a]	800[a]
5NiYZ(i)	4.4	0.6	0.1	67	40	31	29	14	2	80	97	100
5NiYZ	2.0	0.8	0.0	54	50	32	42	14	0	91	96	100
10NiYZ	3.0	0.3	0.0	135	49	28	40	25	4	80	97	100

[a] Temp. (°C).

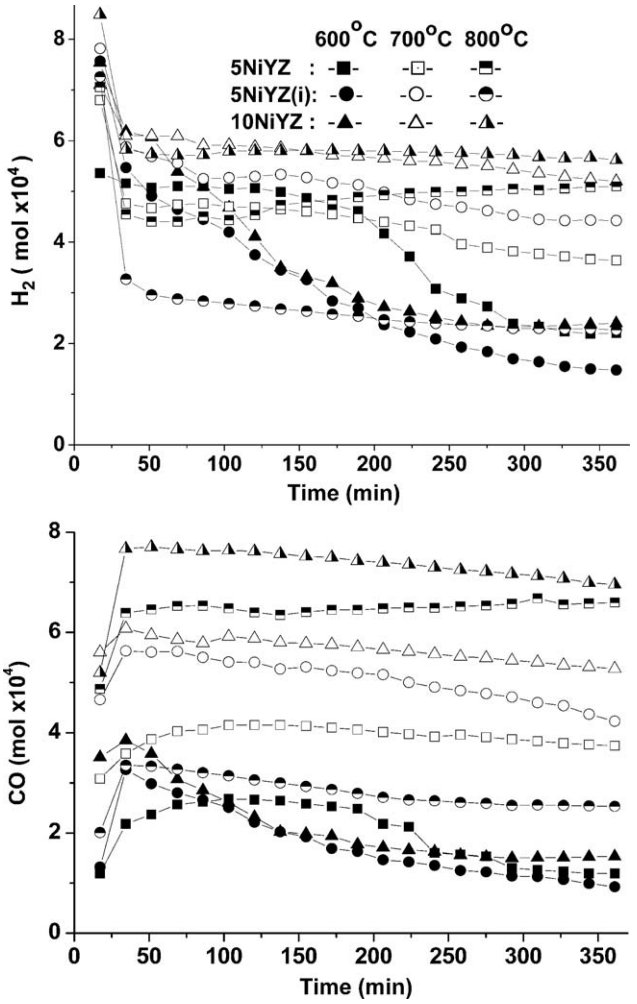

Fig. 5. H_2 (a) and CO (b) mol production of dry reforming of ethanol.

The presence of water is due to the water-gas shift reaction (WGSR: $CO + H_2O \leftrightarrow H_2 + CO_2$) and the dehydration of ethanol to ethene (Fig. 4), the 5NiYZ catalyst showing the least ethene formation at all reaction temperatures. The gaseous product at 600 °C showed most CO_2 conversion on the 10NiYZ catalyst, apparently due to the WGSR, according to the high water production. At this temperature, also, the highest CH_4 is produced on the 5NiYZ catalyst, due to its catalyzing the highest ethanol conversion ($C_2H_5OH \rightarrow CH_4 + H_2 + CO$) with the lowest acetaldehyde selectivity ($C_2H_5OH \rightarrow CH_3CHO + H_2$), and the presence of CH_4 is due to the fact that at 600 °C the dry reforming of CH_4 is slow. At 700 °C and 800 °C the ethanol conversion is practically the same, but the carbon deposition falls sharply on all catalysts at 800 °C, being higher on the 10NiYZ catalyst, due to the greater Ni load. At 700 °C it is observed that the CO_2 conversion is lower and the CH_4 content is higher, on the 5NiYZ(i) catalyst, indicating that the dry reforming of CH_4 occurs with less intensity. At 800 °C, selectivity for the dry reforming of methane increases on all catalysts and more so on the 5NiYZ catalyst, consistently with the CO_2 and CH_4 conversion, and the practically zero carbon deposition. In this catalyst, most of the Ni is interacting with the oxygen vacancies on the support (α peaks in the TPR profiles), while the 5NiYZ(i) and 10NiYZ catalysts show Ni species with less interaction (β peaks in the TPR). As reported by other authors [22,23], the oxygen vacancies may activate the oxygen of the CO_2, catalyzing the removal of carbon deposited on the Ni. This mechanism should occur more easily on the Ni species in more intimate contact with the oxygen vacancies (Ni in α peaks), and this behavior was observed less on 5NiYZ(i), since this catalyst showed more aggregation of NiO, hence less Ni species in close contact with the oxygen vacancies.

4. Conclusions

The synthesis of $Ni/Y_2O_3–ZrO_2$ supported catalysts by polymerization in one step is viable and offers an easier and faster method to deposit Ni on a matrix with negligible NiO solubility, giving more finely dispersed Ni than by wet impregnation. With regard to the dry reforming of ethanol, this reaction occurs in the same range of temperature as the dry reforming of CH_4, so that the CH_4 formed should be reformed in these conditions. The 5NiYZ catalyst gave the best results for this reaction. These indicated that the synthesis method used here was highly practical and led to an efficient catalyst.

References

[1] D.K. Liguras, D.I. Kondarides, X.E. Verykios, Appl. Catal. B 43 (2003) 345–354.
[2] L.V. Mattos, F.B. Noronha, J. Power Sources 145 (2005) 10–15.
[3] M.S. Batista, R.K.S. Santos, E.M. Assaf, J.M. Assaf, E.A. Ticianelli, J. Power Sources 134 (2004) 27–32.
[4] N. Homs, J. Llorca, P. Ramírez de la Piscina, Catal. Today 116 (2006) 361–366.
[5] D.K. Liguras, K. Goundani, X.E. Verykios, J. Power Sources 130 (2004) 30–37.
[6] V. Fierro, V. Klouz, O. Akdim, C. Mirodatos, Catal. Today 75 (2002) 141–144.
[7] J.A. Montoya, E. Romero-Pascual, C. Gimonc, P. Del Angel, A. Monzón, Catal. Today 63 (2000) 71–85.
[8] X. Li, J.-S. Chang, S.-E. Park, Chem. Lett. 28 (1999) 1099–1100.
[9] H.S. Roh, H.S. Potdar, K.W. Jun, Catal. Today 93 (2004) 39–44.
[10] D. Srinivas, C.V.V. Satyanarayana, H.S. Potdar, P. Ratnasamy, Appl. Catal. A 246 (2003) 323–334.
[11] M. Labaki, J.F. Lemonier, S. Siffert, E.A. Zhilinskaya, A. Aboukai, Appl. Catal. B 43 (2003) 261–271.
[12] H. Teterycz, R. Klimkiewwicz, M. Laniecki, Appl. Catal. A 249 (2003) 313–326.
[13] K. Oliveira, N. Abatzoglou, F. Gitzhofer, Can. J. Chem. Eng. 83 (2005) 978–984.
[14] J.D.A. Bellido, E.M. Assaf, Appl. Catal. A 352 (2009) 179–187.
[15] V. Gulia, A.G. Vedeshwar, N.C. Mehra, Acta Mater. 54 (2006) 3899–3905.
[16] P.A. Lessing, Am. Ceram. Soc. Bull. 68 (1989) 1002–1007.
[17] Y.W. Zhang, Z.G. Yan, F.H. Liao, C.S. Liao, C.H. Yan, Mater. Res. Bull. 39 (2004) 1763–1777.
[18] A. Pimenov, J. Ullrich, P. Lunkenheimer, A. Loidl, C.H. Ruscher, Solid State Ionics 109 (1998) 111–118.
[19] A. Kuzjukevics, S. Linderoth, Solid State Ionics 93 (1997) 255–261.
[20] J.M. Howe, Interfaces in Materials—Atomic Structure, Thermodynamics and Kinetics of Solid–Vapor, Solid–Liquid and Solid–Solid Interfaces, John Wiley & Sons, New York, 1997.
[21] W.P. Dow, T.J. Huang, J. Catal. 160 (1996) 155–170.
[22] T.J. Huang, H.J. Lin, T.C. Yu, Catal. Lett. 105 (2005) 239–247.
[23] J.B. Wang, S.Z. Hsiao, T.J. Huang, Appl. Catal. A 246 (2003) 197–211.